The published work can be found in: *Integrated Ferroelectrics*, Vol 51 Issue 1, June 2003 , pages 39 - 49

Pulse-Extended Excimer Laser Crystallisation of Ferroelectric Thin Films for Integration on Low Thermal Budget Substrates

P.P. DONOHUE[1], M.A. TODD[1] and Z. HUANG[2]

[1]QinetiQ Ltd, Malvern Technology Centre, St. Andrews Road, Malvern, Worcestershire, WR14 3PS, UK

[2]Department of Advanced Materials, School of Industrial and Manufacturing Science, Cranfield University, Bedfordshire, MK43 0AL,UK

The use of pulsed laser annealing in ferroelectric device processing is of interest for integration of materials such as lead zirconate titanate (PZT) and strontium bismuth tantalate (SBT) on low thermal budget substrates. Excimer lasers provide a suitable radiation source in a short pulse-duration format with photon energies above the ferroelectric bandgap. Studies with thin film PZT have revealed that standard excimer laser annealing can preferentially heat the ferroelectric layer relative to the substrate but results in severe surface heating and poor heat distribution in this layer. A pulse-extension technique has been used to lengthen the laser pulse duration from 25ns to 374ns, lowering the surface temperature and improving the heat distribution in the PZT but still not significantly heating the substrate. Initial experiments have shown the technique to be capable of crystallising over half a 500nm thick PZT film to perovskite although a melting effect limited the converted thickness. The thickness crystallised is however of the order of that used in FeRAM devices and modelled temperature profiles suggest that the technique provides a tractable solution for high temperature processing of ferroelectric thin films on low thermal budget substrates.

Keywords: Laser annealing, pulse-extension, ferroelectric, thin film.

INTRODUCTION

Excimer lasers are widely used for annealing of thin films of materials that require a higher crystallisation temperature than the substrates on which they sit can withstand. Examples are the crystallisation of a-Si on low thermal budget glass substrates for TFT's in liquid crystal display applications [1, 2], solar cells and IC's on flexible substrates [3]. Some work has been reported on excimer laser annealing of ferroelectric thin films, both cystallisation from an amorphous state [4] and a two step crystallisation process involving combined furnace/laser annealing [5, 6] whereby a low temperature perovskite

phase is initiated by a relatively low temperature and long duration furnace anneal and then refined by laser annealing. This paper details a novel development of excimer laser annealing where the films are annealed from the amorphous state using pulses which have been temporally extended [7, 8]. The extension of the pulse duration (fwhm), from 25ns to 374ns, alleviates two of the main problems of excimer laser annealing of ferroelectric thin films, namely high surface temperatures and poor heat distribution, by increasing the diffusion length of the heat generated during the pulse, while still retaining the benefit of not significantly heating the underlying substrate.

EXPERIMENT

Thin film PZT 30/70 with a 10% Pb excess was deposited using the sol-gel technique [9, 10] onto platinised silicon substrates giving the structure PZT(~500nm)/Pt(1000∑)/Ti(100∑)/SiO_2(0.8µm)/Si. Each PZT layer was fired at 400°C to remove organic components. The optical properties of the as-deposited PZT, used for modelling purposes, were measured using reflectometry and spectroscopic ellipsometry. Laser annealing was accomplished using a bespoke system, described in detail elsewhere [7, 8], comprising a Lambda Physik LPX210 KrF excimer laser (248nm), pulse-extension optics (25ns pulse width to 374ns pulse width), a Microlas beam homogeniser (8mm×8mm uniform beam to ±5%) and a vacuum compatible annealing chamber with heated substrate holder. Temporal pulse shapes were measured using an ITL vacuum photodiode coupled to a Gould 4094 DSO.
The PZT thin films were assessed using X-Ray diffraction (XRD), scanning electron microscopy (SEM), energy dispersive spectroscopy (EDS) and transmission electron microscopy (TEM) techniques. Detailed crystallographic phase investigations were made using small area electron diffraction (SAED) in a Philips CM20 TEM.

TEMPERATURE PROFILE MODELLING

The temperature profiles developed in the thin film layer stacks due to laser irradiation have been predicted by solution of the heat diffusion equation with the addition of a source term for laser induced heating. When a beam homogeniser is used then away from the edge of the illuminated region the heat diffusion problem can be reduced to the unidimensional case since any temperature variation will occur only along an axis perpendicular to the sample surface. Additionally the annealing conditions and materials properties are such that heat flow by radiation, convection and conduction into the surrounding atmosphere can be neglected. The temperature T at distance z from the illuminated surface and time t is then given by

$$\frac{\partial T}{\partial t} = \frac{\alpha}{\rho c_p} I(z,t) + \frac{1}{\rho c_p} \frac{\partial}{\partial z}\left(\kappa \frac{\partial T}{\partial z}\right) \qquad (1)$$

where I is the laser power density, α is the optical absorption coefficient, ρ is the density, c_p is the specific heat capacity and κ is the thermal conductivity. The optical constants of the PZT thin films were determined experimentally and thermal properties for each layer were those determined for bulk materials [11, 12, 13], the layers considered being sufficiently thick for this to be a valid assumption [8]. Due to the complex nature of the samples equation (1) is not solvable analytically. A forward time finite difference approach, described in detail elsewhere [7, 8, 14], has been used to solve for the temperature distribution. The approach adopted involved the layer structure be discritised into finite slices of thickness 50nm, temperatures output being the average for each slice, and time discritised into 25ps units. This numerical approach allowed temperature variation of the layer thermal properties to be taken into account and also measured pulse temporal profiles to be used.

RESULTS

500nm Thick PZT Films

Modelled temperature profiles in the PZT layer stack are shown for the case of a non-extended pulse (fwhm ~ 25ns) in Figures 1 and 2. Figure 1 illustrates the temperatures developed in the PZT slices during and after a pulse of fluence 100mJ/cm^2, assuming an ambient temperature of 300°C. The curve labelled PZT surface is the slice adjacent to the film surface while that labelled PZT/Pt interface is the slice adjacent to the Pt. Figure 2 shows a cross section through the layer stack (the thin Ti adhesion layer has been omitted) at several times after the onset of the pulse. It can be seen from the figures that the non-extended pulse induces very high surface temperatures and large temperature gradients in the PZT – primarily due to the very short absorption length (~20nm at 248nm) and low thermal diffusivity (~5×10^{-7}m^2/s) of this layer. The surface temperature of the PZT reaches a maximum of 1758°C, with the PZT adjacent to the Pt reaching 444°C. Interestingly the uppermost portion of the Si substrate reaches a maximum of only 324°C, only 24°C above ambient, partly due to the thermal barrier action of the SiO_2.

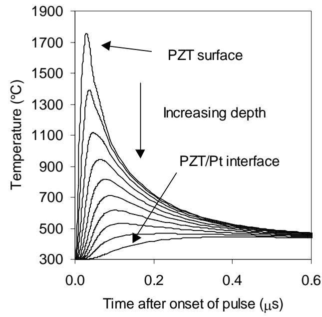

Figure 1: Modelled temperature distribution in a 500nm thick PZT thin film due to non-extended laser pulse of fluence 100mJ/cm^2

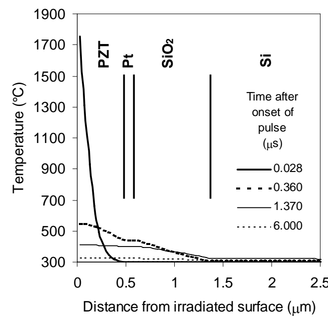

Figure 2: Modelled temperature distribution in layer stack with 500nm thick PZT thin film and non- extended laser pulse of fluence 100mJ/cm^2

Figures 3 and 4 show the same plots for an extended pulse of the same fluence, 100mJ/cm^2. The surface temperature is lower than for the non-extended case, maximum 805°C, while the temperature of the PZT adjacent to the Pt is very similar at 438°C – indicating a better temperature distribution in the PZT layer due to the extended pulse increasing the diffusion length by around factor of four. The extended pulse is still sufficiently short however for the maximum temperature of the topmost Si to only reach 324°C – the same value as for the non-extended case.

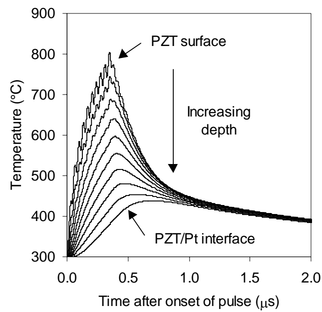

Figure 3: Modelled temperature distribution in a 300nm thick PZT thin film due to an extended laser pulse of fluence 100mJ/cm^2

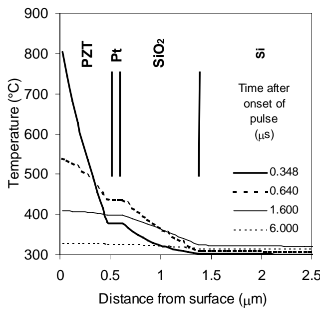

Figure 4: Modelled temperature distribution in layer stack with 500nm thick PZT thin film and extended laser pulse of fluence 100mJ/cm^2

Using the modelled temperature profiles as a guide to the required fluence level PZT thin films were annealed using extended pulses in an O_2

atmosphere with the ambient temperature set to 300°C. Detailed microstructural analysis has been presented previously [7, 8], but the films have, for fluence levels of ~100mJ/cm^2 and less, crystallised to perovskite with no surface damage. The PZT crystal structure, from the top surface down, determined by SAED was perovskite/pyrochlore/amorphous with no perovskite nucleation or growth at the PZT/Pt interface. Table 1 below gives the thickness of the perovskite, pyrochlore and amorphous regions in the PZT for various fluence levels and pulse counts. The thickest perovskite layer was 280nm, over half the original film thickness, and was formed by 10^4 pulses at a fluence of 100mJ/cm^2.

Anneal conditions		Perovskite Region Thickness (nm)	Pyrochlore Region Thickness (nm)	Amorphous Region Thickness (nm)
Number of Pulses	Fluence (mJ/cm^2)			
10^4	80	157	107	221
16×10^4	80	154	100	231
10^4+10^4	80+100	242	99	144
10^4	100	280	81	114

Table 1: Crystallisation thicknesses in pulse-extended laser annealed PZT thin films.

An interesting surface-damage effect was observed when the fluence level was increased above 100mJ/cm^2. Figures 5, 6 and 7 show SEM pictures of sample surfaces at fluence levels of 80mJ/cm^2 (10^4 pulses), 117mJ/cm^2 (10^2 pulses) and 200mJ/cm^2 (10^3 pulses) respectively. At 80mJ/cm^2 the surface is smooth while at 117mJ/cm^2 small pits are starting to appear. Increasing the fluence to 200mJ/cm^2 resulted in dramatic surface disruption and what appears to be a melt pattern. It may be noted that the 117mJ/cm^2 and 200mJ/cm^2 annealed films had the same composition as the as-deposited films and both showed some degree of perovskite crystallisation. Figure 8 shows the modelled maximum temperatures attained at various depths in the PZT at the three fluence levels. Also indicated is the melting temperature of PbO, 886°C, the component in the original film with the lowest melting point. The modelled temperature distributions do not take into account phase changes, such as melting, and should only be considered as a rough guide only. For a fluence of 80mJ/cm^2 the whole PZT film is well below the PbO melting temperature. At 117mJ/cm^2 however the very top of the film has reached the PbO melting temperature, corresponding to small scale pitting in the SEM picture, while at 200mJ/cm^2 this has increased to around half the PZT thickness, corresponding to gross disruption in the annealed film.

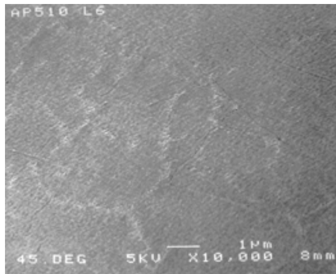

Figure 5: Surface of PZT thin film annealed with extended pulses of fluence 80mJ/cm^2.

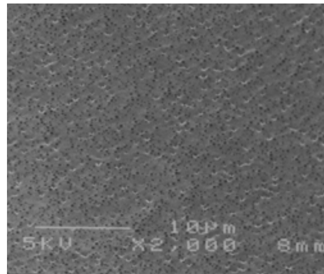

Figure 6: Surface of PZT thin film annealed with extended pulses of fluence 117mJ/cm^2.

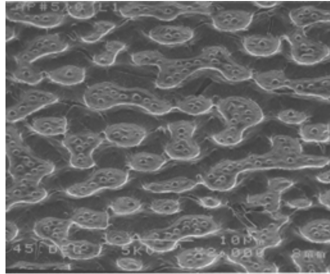

Figure 7: Surface of PZT thin film annealed with extended pulses of fluence 200mJ/cm^2.

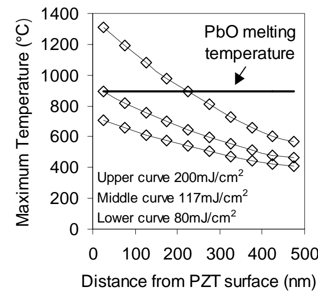

Figure 8: Maximum slice temperature versus extended pulse fluence.

200nm and 300nm Thick PZT Films

Since the pulse-extension technique is limited in the thickness of perovskite PZT that can be crystallised, due to fluence limitations identified in the previous section, thinner layers were modelled to determine the temperature distributions. Figures 9 and 10 show the temperature distribution in a 300nm thick PZT film and in the whole layer stack respectively for an extended pulse of fluence 100mJ/cm^2 and an ambient temperature of 300°C. The temperature distribution in the PZT is seen to be better than for the 500nm thick film with the maximum surface and PZT/Pt interface temperatures being 712°C and 468°C respectively, a difference of 244°C, while the topmost part of the Si only reaches a maximum of 327°C. For a 200nm thick PZT film, Figures 11 and 12, the situation improves further with maximum surface and PZT/Pt interface temperatures being 643°C and 483°C respectively, a difference of only 160°C, while the topmost Si only reached a temperature of 328°C. Compared with the 500nm thick PZT films pulse-extended annealing of these thinner films will benefit from lower surface temperatures and a much improved heat distribution within the PZT film,

without any apparent penalty in laser induced substrate heating. The portion of the PZT film close to the Pt is also getting sufficiently hot for perovskite crystallisation [15].

Since the PZT surface temperatures for the thinner films are distinctly lower than the PbO melting temperature, 253°C lower for the 200nm thick film, there is scope for increasing the fluence and bringing the entire PZT film up to the temperature levels used in the Rapid Thermal Processor (RTP) annealing route without taking the substrate above detrimental temperatures - ~450-500°C for standard Al based CMOS circuitry.

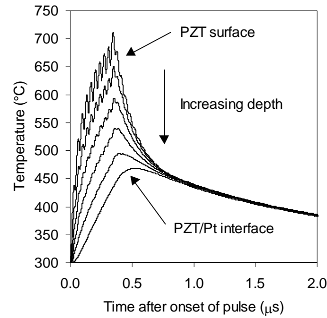

Figure 9: Modelled temperature distribution in a 300nm thick PZT thin film due to an extended laser pulse of fluence 100mJ/cm^2

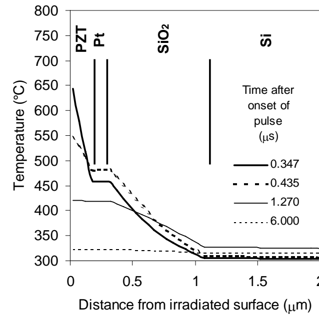

Figure 10: Modelled temperature distribution in layer stack with 300nm thick PZT thin film and extended laser pulse of fluence 100mJ/cm^2

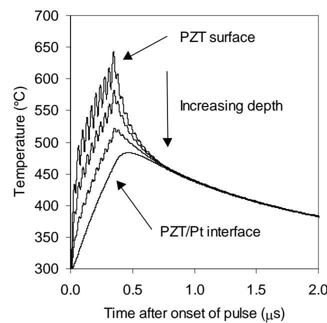

Figure 11: Modelled temperature distribution in a 200nm thick PZT thin film due to an extended laser pulse of fluence 100mJ/cm^2

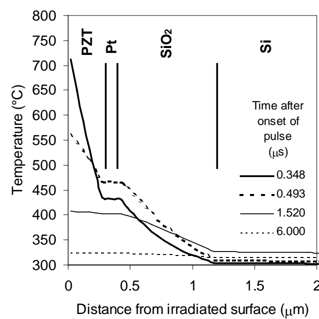

Figure 12: Modelled temperature distribution in layer stack with 200nm thick PZT thin film and extended laser pulse of fluence 100mJ/cm^2

DISCUSSION AND CONCLUSIONS

Low temperature deposited PZT thin films can be crystallised into the perovskite phase using pulse-extended excimer laser annealing. Additionally the temperature rise is largely confined to the ferroelectric layer making the technique suitable for applications which involve low thermal budget substrates, such as FeRAM devices – especially involving SBT films which require very high temperature processing. Compared to annealing with a standard pulse the action of the pulse extender slows down the rate of energy delivery to the PZT, giving lower surface temperatures and improved heat distribution. Use of this technique has been shown to be able to crystallise up to 280nm of an amorphous PZT film to perovskite, which is of the order of the thickness required for ferroelectric based non-volatile memory. The thickness of film that can be crystallised is however limited due to fluence restrictions believed to be due to melting of the PbO component in the as-deposited PZT. Modelling studies have however indicated that for thinner films, of the order of 200-300nm in thickness, the technique should be capable of raising the entire PZT thin films to temperatures used in conventional annealing treatments, e.g. RTP, without detrimentally heating a low thermal budget substrate such as CMOS circuitry.

ACKNOWLEDGEMENTS

This work was funded by the UK Ministry of Defence. The authors gratefully acknowledge the contributions of their colleagues at QinetiQ, Prof. R.W. Whatmore of Cranfield University, Prof. H.N. Rutt of Southampton University and Dr. P. Rumsby of Exitech Ltd. Dr. A. Patel of BAE Systems is thanked for supplying the thin film PZT. © QinetiQ ltd 2002.

REFERENCES

[1] K. Sera, F. Okumura, H. Uchida, S. Itoh, S. Kaneko and K. Hotta, IEEE Trans. on Electron Devices **36**(12), 2868 (1989).
[2] S.D. Brotherton, J.R. Ayres, M.J. Edwards, C.A. Fisher, C. Glaister, J.P. Gowers, D.J. McCulloch and M. Trainor, Thin Solid Films **337**, 188 (1999).
[3] Semiconductor International, August 2001, p40.
[4] U. Varshney, B.D. Eischelberger and R.D. Churchill, Virtual Proceedings of 1996 NSF Design and Manufacturing Grantees Conference.
[5] Y. Zhu, J. Zhu, Y.J. Song and S.B. Desu, Appl. Phys. Lett. **73**(14), 1958 (1998).
[6] Z. Zhang, J. Zhu, D. Su, J. Liu, H. Shen, Y. Wang, L. Kang, J. Zhou, S. Yang and P. Wu, Thin Solid Films **375**, 172 (2000).
[7] P.P. Donohue, PhD Thesis, University of Southampton, 2000.
[8] P.P. Donohue and M.A. Todd, Intetegrated Ferroelectrics **31**, 285 (2000).
[9] A Patel and J Obhi, GEC J. Res. **12**, 141 (1995).

[10] Q. Zhang, R.W. Whatmore, M.E. Vickers and A. Patel, J. Korean Physical Society **32**, S572 (1998).

[11] CRC Handbook of Chemistry and Physics, D R Lide, 76th Ed., CRC Press, 1996

[12] Tables of Physical and Chemical Constants, G.W.C. Kaye and T.H. Laby, 15th Ed., Longman Scientific and Technical, 1993.

[13] PZT Bulk Ceramic Thermal Properties, N.M. Shorrocks, private communication.

[14] P. Baeri, S.U. Campisano, G. Foti and E. Rimini, J. Appl. Phys. **50**(2), 788 (1979).

[15] Ferroelectric Memories, J.F. Scott, Springer, 2000.